PSFC/JA-02-11

Resistive stability of magnetic dipole and other axisymmetric closed field line configurations

Simakov, A.N., Catto, P.J., Ramos, J.J., Hastie, R.J.*

August 2002

Plasma Science and Fusion Center
Massachusetts Institute of Technology
Cambridge, MA 02139 USA

*EURATOM/UKAEA Fusion Association
Culham Science Centre
Abingdon, Oxon, United Kingdom

This work was supported by the U.S. Department of Energy, Grant No. DE-FG02-91ER-54109.

Submitted for publication to *Physics of Plasmas*

Resistive stability of magnetic dipole and other axisymmetric closed field line configurations

Andrei N. Simakov, Peter J. Catto, Jesus J. Ramos, and R. J. Hastie

Massachusetts Institute of Technology, Plasma Science and Fusion Center,

167 Albany Street, Cambridge, Massachusetts 02139

(August 19, 2002)

Abstract

The stability of axisymmetric plasmas confined by a closed poloidal magnetic field is investigated using magnetohydrodynamic equations with anisotropic resistivity and sound waves retained. It is shown that when the system is axially and up-down symmetric and the plasma beta = (plasma pressure/magnetic pressure) is finite, a resistive instability with a growth rate proportional to the cube root of the resistivity exists at the ideal stability boundary for up-down antisymmetric modes. Both the ideal and resistive stability of a Z pinch equilibrium and the point dipole equilibrium of Krasheninnikov, Catto and Hazeltine [Phys. Rev. Lett. **82**, 2689 (1999)] are studied in detail. For a Z pinch, ideal instabilities are found to always dominate over resistive instabilities. For the point dipole, ideal up-down antisymmetric modes are always stable, and the only resistive instabilities permitted have a growth rate proportional to the resistivity times the square of the azimuthal mode number.

I. Introduction

Plasmas confined by axisymmetric closed line poloidal magnetic fields are common both in nature (examples are stellar and planetary magnetospheres) and in the laboratory (Z pinches, field reversed configurations, multipoles and so on). Understanding of the stability properties of such plasmas is therefore important. Unlike tokamaks, where stability is provided by favorable average magnetic field line curvature, many of the closed field line systems have curvature which is unfavorable everywhere. Stability of such systems is provided by plasma and magnetic field compression due to the closed field lines (or to large trapped particle populations).

Recently, a number of articles have been published concerning plasma stability in closed field line systems and, in particular, in a dipolar magnetic field. These articles have in part been stimulated by the Levitated Dipole Experiment[1] (LDX) being constructed at the Massachusetts Institute of Technology, as well as by a general interest in the stability of magnetospheric plasmas. Different approaches have been used depending mainly upon plasma collisionality, the range of frequencies of interest, and the plasma $\beta \equiv$ (plasma pressure/magnetic pressure). These treatments include ideal magnetohydrodynamics[2–4] (MHD), hybrid anisotropic pressure MHD-kinetic theory,[5] and electrostatic[6–9] and electromagnetic[10–13] kinetic theories. Earlier work considered the electrostatic kinetic stability of multipoles.[14]

To the best of our knowledge, the influence of plasma resistivity on stability has not yet been investigated for such systems in detail. Stabilizing and destabilizing properties of the plasma resistivity are widely acknowledged to be important. Resistive modes have been studied for years (see for example the classic Refs. [15–17]), and resistivity frequently leads to instabilities with growth rates proportional to (resistivity)$^{1/3}$. One of the essential features of most of the existing theories is a strong radial localization of these modes in narrow layers about special isolated or "rational" flux surfaces having closed field lines (neighboring field lines are open or "irrational"). However, in closed field line systems all flux surfaces are geometrically equivalent so resistive modes do not have strong radial localization.

In this paper we investigate the stability of axisymmetric closed field line configurations using linearized resistive MHD equations with anisotropic resistivity and coupling to sound waves. By considering the (ideally most unstable) limit of large azimuthal mode numbers it is possible to formulate the problem in terms of a system of two coupled second order differential equations, with appropriate boundary conditions, whose complex eigenvalues are the mode frequencies associated with each flux surface. These equations are derived in Appendix A and discussed in Sec. II. Similar equations, with isotropic plasma resistivity, have been derived in Ref. [18]. The anisotropic equations are then used in Secs. III and IV, respectively, to study the resistive stability of cylindrically symmetric equilibria (i.e. the Z pinch) and of point dipole equilibria.[19] Most of the Z pinch results are obtained analytically, while the point dipole results require numerical solution. The results are summarized in Sec. V.

II. Equations

In order to study the effects of resistivity on the stability of axisymmetric plasma confined by closed poloidal magnetic field lines we use the standard linearized MHD equations (see for example Ref. [20]) with anisotropic resistivity. Recall that the most unstable modes have the largest azimuthal mode numbers n, as demonstrated in Ref. [21] using the ideal MHD energy principle. Therefore, we consider the limit $n \gg 1$ to derive the following system of two coupled second order differential equations for the radial component ξ_ψ of the plasma displacement $\boldsymbol{\xi}$ and a variable, $W \equiv 4\pi\Gamma p \left(\boldsymbol{\nabla} \cdot \boldsymbol{\xi}\right)$, related to the plasma compressibility:

$$\boldsymbol{B}\cdot\boldsymbol{\nabla}\left[\frac{\left(\boldsymbol{B}\cdot\boldsymbol{\nabla}\xi_\psi\right)}{R^2B^2\left(1+c^2n^2\eta_\parallel/4\pi R^2\gamma\right)}\right]+2\left(\frac{\boldsymbol{\kappa}\cdot\boldsymbol{\nabla}\psi}{R^2B^2}\right)\left(4\pi\frac{\mathrm{d}p}{\mathrm{d}\psi}\xi_\psi+W\right)=\frac{4\pi\rho\gamma^2}{R^2B^2}\xi_\psi, \quad (1)$$

$$\boldsymbol{B}\cdot\boldsymbol{\nabla}\left(\frac{\boldsymbol{B}\cdot\boldsymbol{\nabla}W}{B^2}\right)-2\frac{c^2n^2\eta_\parallel}{\gamma}\frac{\mathrm{d}p}{\mathrm{d}\psi}\left(\frac{\boldsymbol{\kappa}\cdot\boldsymbol{\nabla}\psi}{R^2B^2}\right)\left(4\pi\frac{\mathrm{d}p}{\mathrm{d}\psi}\xi_\psi+W\right)=$$

$$\frac{\rho\gamma^2}{\Gamma p}\left[1+\frac{4\pi\Gamma p}{B^2}\left(1+\frac{c^2n^2\eta_\perp}{4\pi R^2\gamma}\right)\right]W+4\pi\rho\gamma^2\left[2\left(\frac{\boldsymbol{\kappa}\cdot\boldsymbol{\nabla}\psi}{R^2B^2}\right)+\frac{c^2n^2\left(\eta_\perp-\eta_\parallel\right)}{\gamma R^2B^2}\frac{\mathrm{d}p}{\mathrm{d}\psi}\right]\xi_\psi. \quad (2)$$

Here and elsewhere, the equilibrium magnetic field is $\boldsymbol{B} = \boldsymbol{\nabla}\psi \times \boldsymbol{\nabla}\zeta$ with ψ the poloidal magnetic flux and ζ the toroidal coordinate, $\boldsymbol{\kappa} \equiv \hat{\boldsymbol{n}} \cdot \boldsymbol{\nabla} \hat{\boldsymbol{n}}$ is the magnetic field curvature with $\hat{\boldsymbol{n}} \equiv \boldsymbol{B}/B$, R is a cylindrical radial coordinate, p and ρ are plasma pressure and density, respectively, $\Gamma \equiv c_p/c_v$ is the ratio of specific heats at constant pressure and volume, $\eta_{\|}$ and $\eta_{\perp}$ are parallel and perpendicular resistivities, γ is the mode growth rate, and c is the speed of light. The quantities $\eta_{\|,\perp}$ and ρ are assumed to be functions of ψ only. Details of the derivation of Eqs. (1) and (2) are given in the Appendix A. When deriving these equations it is assumed that $\left(c^2\eta_{\|,\perp}/4\pi R^2\gamma\right) \ll 1$ while $\left(c^2 n^2\eta_{\|,\perp}/4\pi R^2\gamma\right) = \mathrm{O}\left(1\right)$. The quantity W describes plasma compression which has a stabilizing influence and must be retained to properly treat resistive modes.[16,17] These equations describe shear Alfvén modes, sound waves, and resistive modes, and must be solved on each flux surface $\psi =$ constant to obtain the corresponding eigenfunctions and eigenvalues, which are complex frequencies local to each surface.

The system of coupled differential equations (1) and (2) can be greatly simplified in the case of ideal modes ($\eta_{\|} = \eta_{\perp} = 0$) near marginality. Notice from Eq. (2) that the variation of W along $\boldsymbol{B}$ is proportional to γ^2, so as $\gamma \to 0$, W becomes a flux function. Therefore, it follows by field line averaging Eq. (2) that

$$W \approx -8\pi\Gamma p \frac{\left\langle \xi_\psi \left(\boldsymbol{\kappa} \cdot \boldsymbol{\nabla}\psi\right)/R^2B^2 \right\rangle_\theta}{1 + 4\pi\Gamma p \left\langle B^{-2} \right\rangle_\theta}, \tag{3}$$

so that Eq. (1) becomes

$$R^2B^2\boldsymbol{B} \cdot \boldsymbol{\nabla} \left(\frac{\boldsymbol{B} \cdot \boldsymbol{\nabla}\xi_\psi}{R^2B^2} \right) + 4\pi \left[2\left(\boldsymbol{\kappa} \cdot \boldsymbol{\nabla}p\right) - \rho\gamma^2 \right] \xi_\psi = \\ 16\pi\Gamma p \left(\boldsymbol{\kappa} \cdot \boldsymbol{\nabla}\psi\right) \frac{\left\langle \xi_\psi \left(\boldsymbol{\kappa} \cdot \boldsymbol{\nabla}\psi\right)/R^2B^2 \right\rangle_\theta}{1 + 4\pi\Gamma p \left\langle B^{-2} \right\rangle_\theta}. \tag{4}$$

Here, $\langle \ldots \rangle_\theta$ denotes the field line average, $\langle \ldots \rangle_\theta \equiv V^{-1} \oint \left[\left(\ldots\right) \mathrm{d}\theta/\boldsymbol{B} \cdot \boldsymbol{\nabla}\theta \right]$, with $V \equiv \oint \left[\mathrm{d}\theta/\boldsymbol{B} \cdot \boldsymbol{\nabla}\theta \right]$ and θ the poloidal angle. Equation (4) is the well-known ballooning equation for shear Alfvén modes which can be derived from the ideal MHD energy principle. The four terms of Eq. (4) (from left to right) correspond to the magnetic field line bending energy (stabilizing), the curvature instability drive due to a pressure gradient, the plasma inertia and the plasma and magnetic field compression energy (stabilizing). This equation has been obtained for example in Refs. [18,21] and its solutions for the point dipole equilibrium[19] have been discussed in detail in Ref. [3]. The fact that sound waves do not enter when the energy principle is used implies that they are always ideally stable.

The first terms of Eqs. (1) and (4) are identical except that the former is $\left(1 + c^2 n^2 \eta_{\|}/4\pi R^2 \gamma\right)$ times smaller than the latter. This change represents the fact that parallel resistivity allows plasma to "slip" through magnetic field lines, effectively reducing the stabilizing field line bending energy, which may result in an instability. The physical meaning of the resistive terms in Eq. (2) is not so obvious. Evidently, some of them correspond to a resistive dissipation of energy, while others seem to describe the decrease in the perturbed pressure due to plasma "slipping" through the magnetic field.

The resistive time $\tau_{res} \equiv (4\pi R^2/c^2 n^2 \eta)$ is usually much larger than the Alfvén time $\tau_A \equiv \sqrt{4\pi \rho R^2/B^2}$. For example, for LDX plasmas with density $N \sim 10^{13}\,\mathrm{cm}^{-3}$, temperatures $T_e \sim T_i \sim 100\,\mathrm{eV}$, magnetic field $B \sim 2\,\mathrm{kG}$, and characteristic dimensions $R \sim 1\,\mathrm{m}$ we find $\tau_A \sim 7 \times 10^{-7}\,\mathrm{sec}$, $\tau_{res} \sim 1.5 n^{-2}\,\mathrm{sec}$ so that $(\tau_A/\tau_{res}) \sim 5 \times 10^{-7} n^2$, where the upper bound on n is given by an MHD applicability condition $k_\perp \rho_i < 1$, resulting in the estimate $n < 200$. Here, $k_\perp \sim n/R$ is the azimuthal wave number and ρ_i is the ion gyroradius. Consequently, for the LDX plasmas $(\tau_A/\tau_{res}) < 2 \times 10^{-2} \ll 1$. Therefore, we may expect that resistivity, which always enters Eqs. (1) and (2) in the combination $(1/\tau_{res}\gamma)$, can lead to resistive modifications in two different ways: (i) small resistive corrections of order τ_{res}^{-1} to otherwise stable ideal MHD modes away from ideal stability boundaries; and (ii) strong resistive instabilities which occur only near ideal MHD stability boundaries, where γ is small so even a small decrease in stabilizing field line bending becomes important. In the remainder of this section we will demonstrate that case (ii) leads to a strong resistive instability with $\gamma \propto \eta_{\|}^{1/3}$, while in Secs. III and IV we will give examples, which show that case (i) results in weaker modes with $\mathrm{Re}\,(\gamma) \propto \tau_{res}^{-1} \propto \eta$. Notice that we define the resistive time scale of interest, τ_{res}, to be n^2 times faster than the equilibrium resistive evolution time scale, which is of order $(4\pi R^2/c^2\eta)$.

To demonstrate $\gamma \propto \eta_{\|}^{1/3}$ growth, we consider closed field line toroidal systems which are not only axisymmetric, but also up-down symmetric (for example, magnetic dipoles), so that all modes are up-down symmetric (even) or antisymmetric (odd). Using Eqs. (1) and (2), we will next show that in such toroidal systems, if the ideal odd mode can become marginally stable and $\langle (\boldsymbol{B}\cdot\boldsymbol{\nabla}\xi_\psi)/R^2\rangle_\theta \neq 0$, an unstable resistive mode with growth rate $\gamma \propto \eta_\parallel^{1/3}$ always exists for $\beta \sim 1$. There are no corresponding resistive modes at the stability boundary for the ideal interchange mode (the least stable even mode).

We begin by assuming that, in the vicinity of an ideal marginal point, $\gamma \sim \tau_A^{-2/3}\tau_{res}^{-1/3} \propto \eta^{1/3}$ and $\beta \sim 1$, so that $(1/\tau_{res}\gamma) \sim \gamma^2\tau_A^2 \sim (\tau_A/\tau_{res})^{2/3} \equiv \delta \ll 1$. We then expand ξ_ψ and W in powers of δ,

$$\xi_\psi = \xi_{\psi 0} + \delta\,\xi_{\psi 1} + \delta^2\,\xi_{\psi 2} + \dots\ ,$$
$$W = W_0 + \delta\,W_1 + \delta^2\,W_2 + \dots\ .$$

Focusing on the odd modes and using the preceding expansions, it is easy to solve Eqs. (1) and (2) order by order. Thus, Eq. (2) gives to leading order

$$\boldsymbol{B}\cdot\boldsymbol{\nabla}\left(\frac{\boldsymbol{B}\cdot\boldsymbol{\nabla}W_0}{B^2}\right) = 0, \tag{5}$$

which, together with periodicity of W_0 along a field line, requires $W_0 = W_0(\psi)$, so for an odd solution $W_0 = 0$. Then, Eq. (2) gives to next order

$$\boldsymbol{B}\cdot\boldsymbol{\nabla}\left(\frac{\boldsymbol{B}\cdot\boldsymbol{\nabla}W_1}{B^2}\right) = 8\pi\left[\rho\gamma^2 + \frac{c^2n^2\eta_\parallel}{\gamma}\left(\frac{\mathrm{d}p}{\mathrm{d}\psi}\right)^2\right]\left(\frac{\boldsymbol{\kappa}\cdot\boldsymbol{\nabla}\psi}{R^2B^2}\right)\xi_{\psi 0}. \tag{6}$$

Using the leading order form of Eq. (1),

$$\boldsymbol{B}\cdot\boldsymbol{\nabla}\left(\frac{\boldsymbol{B}\cdot\boldsymbol{\nabla}\xi_{\psi 0}}{R^2B^2}\right) + 8\pi\frac{\mathrm{d}p}{\mathrm{d}\psi}\left(\frac{\boldsymbol{\kappa}\cdot\boldsymbol{\nabla}\psi}{R^2B^2}\right)\xi_{\psi 0} = 0, \tag{7}$$

in Eq. (6) we obtain

$$\boldsymbol{B}\cdot\boldsymbol{\nabla}W_1 + \left(\frac{\rho\gamma^2}{\mathrm{d}p/\mathrm{d}\psi} + \frac{c^2n^2\eta_\parallel}{\gamma}\frac{\mathrm{d}p}{\mathrm{d}\psi}\right)\left(\frac{\boldsymbol{B}\cdot\boldsymbol{\nabla}\xi_{\psi 0}}{R^2}\right) = K(\psi)\,B^2, \tag{8}$$

where the flux function $K(\psi)$ can be determined by field line averaging Eq. (8):

$$K(\psi) = \left(\frac{\rho\gamma^2}{\mathrm{d}p/\mathrm{d}\psi} + \frac{c^2n^2\eta_\parallel}{\gamma}\frac{\mathrm{d}p}{\mathrm{d}\psi}\right)\left\langle\frac{\boldsymbol{B}\cdot\boldsymbol{\nabla}\xi_{\psi 0}}{R^2}\right\rangle_\theta\frac{1}{\langle B^2\rangle_\theta}. \tag{9}$$

Equations (8) and (9) give then

$$\boldsymbol{B}\cdot\boldsymbol{\nabla}\left(\frac{\boldsymbol{B}\cdot\boldsymbol{\nabla}W_1}{R^2B^2}\right)=\left(\frac{\rho\gamma^2}{\mathrm{d}p/\mathrm{d}\psi}+\frac{c^2n^2\eta_\parallel}{\gamma}\frac{\mathrm{d}p}{\mathrm{d}\psi}\right) \tag{10}$$
$$\times\left[\boldsymbol{B}\cdot\boldsymbol{\nabla}\left(\frac{1}{R^2}\right)\frac{\left\langle\left(\boldsymbol{B}\cdot\boldsymbol{\nabla}\xi_{\psi 0}\right)/R^2\right\rangle_\theta}{\left\langle B^2\right\rangle_\theta}-\boldsymbol{B}\cdot\boldsymbol{\nabla}\left(\frac{\boldsymbol{B}\cdot\boldsymbol{\nabla}\xi_{\psi 0}}{R^4B^2}\right)\right].$$

Finally, using Eq. (10) together with the next order version of Eq. (1),

$$\boldsymbol{B}\cdot\boldsymbol{\nabla}\left(\frac{\boldsymbol{B}\cdot\boldsymbol{\nabla}\xi_{\psi 1}}{R^2B^2}\right)+2\left(\frac{\boldsymbol{\kappa}\cdot\boldsymbol{\nabla}\psi}{R^2B^2}\right)\left(4\pi\frac{\mathrm{d}p}{\mathrm{d}\psi}\xi_{\psi 1}+W_1\right) \tag{11}$$
$$=\frac{c^2n^2\eta_\parallel}{4\pi\gamma}\boldsymbol{B}\cdot\boldsymbol{\nabla}\left(\frac{\boldsymbol{B}\cdot\boldsymbol{\nabla}\xi_{\psi 0}}{R^4B^2}\right)+\frac{4\pi\rho\gamma^2}{R^2B^2}\xi_{\psi 0},$$

and introducing a quantity $X\equiv\xi_{\psi 1}+\left[W_1/\left(4\pi\,\mathrm{d}p/\mathrm{d}\psi\right)\right]$, we obtain

$$\boldsymbol{B}\cdot\boldsymbol{\nabla}\left(\frac{\boldsymbol{B}\cdot\boldsymbol{\nabla}X}{R^2B^2}\right)+8\pi\frac{\mathrm{d}p}{\mathrm{d}\psi}\left(\frac{\boldsymbol{\kappa}\cdot\boldsymbol{\nabla}\psi}{R^2B^2}\right)X=\frac{c^2n^2\eta_\parallel}{4\pi\gamma\left\langle B^2\right\rangle_\theta}\left\langle\frac{\boldsymbol{B}\cdot\boldsymbol{\nabla}\xi_{\psi 0}}{R^2}\right\rangle_\theta\boldsymbol{B}\cdot\boldsymbol{\nabla}\left(\frac{1}{R^2}\right) \tag{12}$$
$$+\rho\gamma^2\left\{\frac{4\pi\xi_{\psi 0}}{R^2B^2}+\frac{1}{4\pi\left(\mathrm{d}p/\mathrm{d}\psi\right)^2}\boldsymbol{B}\cdot\boldsymbol{\nabla}\left[\left\langle\frac{\boldsymbol{B}\cdot\boldsymbol{\nabla}\xi_{\psi 0}}{R^2}\right\rangle_\theta\frac{1}{R^2\left\langle B^2\right\rangle_\theta}-\left(\frac{\boldsymbol{B}\cdot\boldsymbol{\nabla}\xi_{\psi 0}}{R^4B^2}\right)\right]\right\}.$$

Multiplying Eq. (12) by $\xi_{\psi 0}$, averaging along the field line, noticing that the operator acting on X on the left-hand side of the equation is self-adjoint, and taking Eq. (7) into account, we arrive at the following expression for the growth rate near the odd mode marginal stability boundary:

$$\gamma=\left[\frac{c^2n^2\eta_\parallel}{\rho}\left(\frac{\mathrm{d}p}{\mathrm{d}\psi}\right)^2F^{-1}\right]^{1/3}, \tag{13}$$

where

$$F\equiv\left[\frac{\left\langle B^2\right\rangle_\theta\left\langle\left(\boldsymbol{B}\cdot\boldsymbol{\nabla}\xi_{\psi 0}\right)^2/R^4B^2\right\rangle_\theta}{\left\langle\left(\boldsymbol{B}\cdot\boldsymbol{\nabla}\xi_{\psi 0}\right)/R^2\right\rangle_\theta^2}-1\right]+\left(4\pi\frac{\mathrm{d}p}{\mathrm{d}\psi}\right)^2\frac{\left\langle B^2\right\rangle_\theta\left\langle\xi_{\psi 0}^2/R^2B^2\right\rangle_\theta}{\left\langle\left(\boldsymbol{B}\cdot\boldsymbol{\nabla}\xi_{\psi 0}\right)/R^2\right\rangle_\theta^2} \tag{14}$$

is a positive quantity. It follows from a Schwarz inequality that the expression in the square brackets is always non-negative. The MHD applicability condition for expression (13), $\gamma\sim\tau_A^{-2/3}\tau_{res}^{-1/3}>\omega_*$, with $\omega_*\sim\left(ck_\perp RT/eN\right)\left(\mathrm{d}N/\mathrm{d}\psi\right)$ the diamagnetic drift frequency and e the magnitude of the electron charge, is easily satisfied for LDX plasmas when $k_\perp\rho_i<1$ is satisfied.

Therefore, except for the special case $\left\langle\left(\boldsymbol{B}\cdot\boldsymbol{\nabla}\xi_{\psi 0}\right)/R^2\right\rangle_\theta=0$, a strong resistive instability always exists at the ideal odd mode stability boundary in an axisymmetric and up-down symmetric closed field line configuration for $\beta\sim 1$. Notice that

$\langle (\boldsymbol{B} \cdot \boldsymbol{\nabla} \xi_{\psi 0}) / R^2 \rangle_\theta = 0$ for the cylindrical Z pinch so a resistive instability (at finite β), with $\gamma \propto \eta_\parallel^{1/3}$, does not appear in this case.

It is possible to understand the nature of the above instability from elementary considerations. We consider an axially and up-down symmetric system and assume a plasma perturbation in the form $\xi_\psi (\psi, \theta) \, \mathrm{e}^{-in\zeta}$. Electrons and ions move toroidally in the opposite directions as a result of ∇B and curvature drifts, which causes plasma polarization and generates an axial electric field. The direction of the electric field is such that the corresponding $\boldsymbol{E} \times \boldsymbol{B}$ drift enhances the perturbation. Instability occurs if the stabilizing effects of plasma compressibility and/or the field line bending are weak enough. Notice that the larger n, the stronger the generated electric field and, consequently, the instability.

Next, we consider an up-down antisymmetric (odd) perturbation at its ideal stability boundary. If $\eta_\parallel = 0$, the perturbation simply sits there, prevented from growing by the magnetic field line bending. If, however, $\eta_\parallel > 0$, plasma slowly diffuses across the field and the perturbation grows, with a growth rate given by Eqs. (13) and (14). The scaling of this growth rate with $\eta_\parallel$ can be approximately understood by looking at Eq. (4). The right-hand side of this equation is approximately zero for odd modes, while the field-line bending term cancels the curvature drive to leading order at the odd mode ideal stability boundary. Then, the resistive correction to the field line bending term, which is roughly equal to the line bending term itself times $(-c^2 n^2 \eta_\parallel / 4\pi R^2 \gamma)$, balances the inertial term, proportional to γ^2, leading to the growth rate $\gamma \propto \eta_\parallel^{1/3}$.

The preceding picture is, of course, greatly simplified, as we haven't accounted for the fact that the diffusion of plasma across the magnetic field due to $\eta_\parallel$ (mainly in the constant ζ plane) can also have a stabilizing influence. This stabilizing effect is described in our case by W_1, a stabilizing compression (or rarefication) of plasma that reduces plasma perturbations. It happens that for Z pinch geometry, $\langle (\boldsymbol{B} \cdot \boldsymbol{\nabla} \xi_{\psi 0}) / R^2 \rangle_\theta = 0$ and these stabilizing and destabilizing effects due to $\eta_\parallel$ exactly cancel for finite β, causing $\gamma \to 0$. In all the other plasma configurations the destabilizing effect of parallel resistivity wins over the stabilizing effect and the $\eta_\parallel^{1/3}$

resistive instability occurs if ideal marginality is accessible.

Considering the case of even modes in a similar way, it is possible to show that there is no resistive instability at the lowest ideal even mode stability boundary for $\beta \sim 1$. The latter result is clear as the lowest and least stable ideal even mode is a flute at the marginal stability boundary so that the field line bending energy vanishes and can play no role in altering stability.

We have just proven from very general considerations that resistive instabilities with growth rates proportional to $\eta_{\|}^{1/3}$ always exist at the ideal odd mode stability boundary (if it is accessible) in axisymmetric and up-down symmetric finite β plasmas confined by closed poloidal magnetic field lines, except for a Z pinch.

In practice, it is possible and desirable to avoid this strong $\eta_{\|}^{1/3}$ resistive growth. It does not occur in the Z pinches because $\langle (\boldsymbol{B} \cdot \boldsymbol{\nabla} \xi_{\psi 0}) / R^2 \rangle_\theta = 0$. More interestingly, it can be avoided in magnetic configurations where ideal odd mode marginality is not accessible. Such a situation occurs for the point dipole equilibrium.[19]

In the next section we consider the Z pinch further to demonstrate that only resistive growth on the τ_{res} time scale may be of concern. In Sec. IV we consider the point dipole configuration in detail. We again find that resistivity only leads to instabilities with growth on the τ_{res} time scale.

III. Resistive Stability of a Z pinch Equilibrium

In this section we study resistive MHD modes for a Z pinch. This problem is briefly considered here as it provides important insights into the general problem since most of the results can be obtained analytically because all equilibrium quantities are constant along field lines.

The system of Eqs. (1) and (2) greatly simplifies in this case as the operator $(\boldsymbol{B} \cdot \boldsymbol{\nabla})$ is simply $(\mathrm{i}\, m\, B/R)$, with m the azimuthal mode number, leading to the dispersion relation

$$\tilde{\gamma}^2 \left\{ \left(\tilde{\gamma}^2 + \frac{m^2 \tilde{\gamma}}{\tilde{\gamma} + \tilde{\eta}_\parallel} \right) \left[1 + \Delta \left(1 + \frac{\tilde{\eta}_\perp}{\tilde{\gamma}} \right) \right] + \Delta \left(4 + m^2 \right) - \alpha \left(1 + \Delta \right) \right\} + \Delta \frac{m^2 \left(m^2 - \alpha \right) \tilde{\gamma}}{\tilde{\gamma} + \tilde{\eta}_\parallel} = 0, \tag{15}$$

with $\tilde{\gamma} \equiv \gamma/\gamma_A$, $\gamma_A \equiv \sqrt{B^2/4\pi\rho R^2}$, $\Delta \equiv \Gamma\beta/2$, $\beta \equiv 8\pi p/B^2$, $\alpha \equiv -\beta \left(\mathrm{d} \ln p / \mathrm{d} \ln R \right)$, and $\tilde{\eta}_{\parallel,\perp} \equiv \left(c^2 n^2 \eta_{\parallel,\perp} / 4\pi R^2 \gamma_A \right)$. Of course, the dispersion relation (15) is a fourth order polynomial equation in $\tilde{\gamma}$ so its exact analytical solution can in principle be written down. However, this solution is hard to analyze and provides little insight, so we instead obtain approximate solutions by considering the most interesting limiting cases. Noticing that the modes with $m = 0$ and those with $m \neq 0$ behave quite differently and do not interact, we proceed by considering them separately.

A. Modes with $m = 0$

Considering modes with $m = 0$, which are equivalent to interchange modes in a more general up-down symmetric equilibrium, Eq. (15) becomes

$$\tilde{\gamma}^2 \left[\left(1 + \Delta \right) \tilde{\gamma}^2 + \tilde{\eta}_\perp \Delta \tilde{\gamma} + 4\,\Delta - \alpha \left(1 + \Delta \right) \right] = 0. \tag{16}$$

This equation has four roots,

$$\tilde{\gamma}_{1,2} = 0, \qquad \tilde{\gamma}_{3,4} = \frac{-\tilde{\eta}_\perp \Delta \pm \sqrt{\tilde{\eta}_\perp^2 \Delta^2 + 4 \left(1 + \Delta \right)^2 \left(\alpha - \frac{4\,\Delta}{1+\Delta} \right)}}{2 \left(1 + \Delta \right)}, \tag{17}$$

where $\tilde{\gamma}_{1,2} = 0$ correspond to the absence of interchange sound waves, while $\tilde{\gamma}_{3,4}$ are interchange shear Alfvén modes. It is clear that stability requires

$$\alpha < 4\,\Delta / \left(1 + \Delta \right). \tag{18}$$

The stability condition (18) for the $m = 0$ mode, obtained first by Kadomtsev[22] from the MHD energy principle, is equivalent to the usual interchange stability condition (see for example Ref. [[23]]),

$$-\mathrm{d} \ln p / \mathrm{d} \ln V < \Gamma. \tag{19}$$

It follows from Eq. (17) that parallel resistivity plays no role in the stability of the $m = 0$ modes in a Z pinch; while perpendicular resistivity does not change the stability boundary, decreases the growth rate of an ideally unstable mode, and damps an ideally stable mode.

B. Modes with $m \neq 0$

Next, we consider modes with $m \neq 0$. Dropping the resistive terms in Eq. (15) for the moment, we find that four ideal modes are present in the system with frequencies

$$\tilde{\gamma}_{1,2,3,4} = \pm\sqrt{\frac{-a \pm \sqrt{a^2 + b}}{2\,(1 + \Delta)}}, \tag{20}$$

where $a \equiv 4\,\Delta + m^2\,(1 + 2\,\Delta) - \alpha\,(1 + \Delta)$ and $b \equiv 4m^2\Delta\,(1 + \Delta)\,(\alpha - m^2)$, so that $a^2 + b = \left[m^2 - \alpha\,(1 + \Delta) + 4\Delta\right]^2 + 16m^2\Delta^2 > 0$. It follows from Eq. (20) that one of the modes is unstable when $\alpha > m^2$ ($b > 0$), while all four of them are stable otherwise. Consequently, in the ideal case for $m \neq 0$ modes stability requires

$$\alpha < m^2. \tag{21}$$

This stability condition has also been derived by Kadomtsev[22] from the MHD energy principle and is discussed in detail in Ref. [[20]]. In particular, it can be shown[20] that the inner core of a Z pinch is always unstable with respect to the $m = 1$ mode except perhaps when a current carrying wire is placed along the axis (hard core Z pinch).

The four modes are strongly coupled at $\beta \sim 1$, but decouple for $\beta \ll 1$, forming two independent sets of (i) sound waves with frequencies (the "+" sign under the square root in Eq. (20))

$$\tilde{\gamma}_{1,2} = \pm \mathrm{i} m\sqrt{\Delta}, \tag{22}$$

and (ii) shear Alfvén modes with frequencies (the "-" sign under the square root in Eq. (20))

$$\tilde{\gamma}_{3,4} = \pm \mathrm{i}\sqrt{m^2 - \alpha}. \tag{23}$$

When deriving expressions (22) and (23) we assume that $1 \sim \alpha \gg \Delta$. As expected, one of the Alfvén modes is unstable when $\alpha > m^2$, while the sound waves are always stable.

Assuming now that the resistivity is small, $\tilde{\eta}_\parallel, \tilde{\eta}_\perp \ll 1$, resistive corrections to the frequencies (20) can easily be obtained perturbatively. For the case of finite Δ and $|m^2 - \alpha|$ the resulting expressions are

$$\tilde{\gamma}_{1,2} = \pm\sqrt{\frac{-a + \sqrt{a^2+b}}{2\,(1+\Delta)}} - \frac{\tilde{\eta}_\parallel}{4}\,(1-d) - \frac{\tilde{\eta}_\perp}{4}\frac{\Delta}{1+\Delta}\,(1+d)\,, \tag{24}$$
$$\tilde{\gamma}_{3,4} = \pm\sqrt{\frac{-a - \sqrt{a^2+b}}{2\,(1+\Delta)}} - \frac{\tilde{\eta}_\parallel}{4}\,(1+d) - \frac{\tilde{\eta}_\perp}{4}\frac{\Delta}{1+\Delta}\,(1-d)\,,$$

with $d \equiv \left[m^2 + \alpha\,(1+\Delta) - 4\Delta\right] / \sqrt{\left[m^2 - \alpha\,(1+\Delta) + 4\Delta\right]^2 + 16 m^2 \Delta^2}$. When the ideal modes are stable, it follows from Eq. (24) that the resistive terms are destabilizing when $|d| > \left[(1+\Delta)\,\tilde{\eta}_\parallel + \Delta\tilde{\eta}_\perp\right] / |\,(1+\Delta)\,\tilde{\eta}_\parallel - \Delta\tilde{\eta}_\perp| \geq 1$, but otherwise result in damping. Noticing that d can be rewritten in the form $d = \left[m^2 + \alpha\,(1+\Delta) - 4\Delta\right] / \sqrt{\left[m^2 + \alpha\,(1+\Delta) - 4\Delta\right]^2 + 4m^2\,(1+\Delta)\,(4\Delta - \alpha)}$, we see that the necessary condition for resistive stability, $|d| < 1$, is equivalent to the requirement $\alpha < 4\Delta$, which is less restrictive than the $m = 0$ interchange stability condition (18). Therefore, interchange stability necessarily implies resistive stability for $m \neq 0$ modes in a Z pinch.

Finally, we consider $m \neq 0$ modes at the ideal stability boundary, $\alpha = m^2$, to test our earlier predictions (see Sec. II) that strong resistive instabilities with $\tilde{\gamma} \propto \tilde{\eta}^{1/3}$ are not possible at finite pressure. In this case, the general dispersion relation (15) becomes a cubic,

$$\begin{aligned}(1+\Delta)\tilde{\gamma}^3 + \left[\tilde{\eta}_\parallel + \left(\tilde{\eta}_\parallel + \tilde{\eta}_\perp\right)\Delta\right]\tilde{\gamma}^2 \\ + \left(4+m^2\right)\Delta\tilde{\gamma} + \left[\left(4\tilde{\eta}_\parallel + m^2\tilde{\eta}_\perp\right)\Delta - m^2\tilde{\eta}_\parallel\right] = 0,\end{aligned} \tag{25}$$

which can be solved perturbatively for $\tilde{\eta}_\parallel, \tilde{\eta}_\perp \ll 1$ to give

$$\tilde{\gamma}_1 = \frac{m^2 - 4\Delta}{(4+m^2)\,\Delta}\,\tilde{\eta}_\parallel - \frac{m^2}{4+m^2}\,\tilde{\eta}_\perp, \tag{26}$$
$$\tilde{\gamma}_{2,3} = \pm\,\mathrm{i}\sqrt{\frac{(4+m^2)\,\Delta}{1+\Delta}} - \frac{m^2\,(1+\Delta)}{2\,(4+m^2)\,\Delta}\,\tilde{\eta}_\parallel + \frac{m^2 - 4\Delta}{2\,(4+m^2)\,(1+\Delta)}\tilde{\eta}_\perp.$$

Therefore, *at finite* Δ, resistivity results in growth or damping rates $\gamma \sim 1/\tau_{res} \propto n^2\eta_{\|,\perp}$. Even though Eq. (25) predicts a strong resistive instability with $\tilde{\gamma} = m^{2/3}\tilde{\eta}_{\|}^{1/3}$ when $\Delta \ll m^{4/3}\tilde{\eta}_{\|}^{2/3}/\left(m^2+4\right) \ll 1$, it is not of concern because the interchange mode is also unstable in this situation and has a growth rate $\tilde{\gamma} = \sqrt{\alpha} = m \gg m^{2/3}\tilde{\eta}_{\|}^{1/3}$, as follows from Eq. (17).

IV. Resistive Stability of the Point Dipole Equilibrium

Although having the great advantage of analytic tractability, Z pinch equilibria represent only a rather special class of plasma equilibria confined by closed line magnetic fields as all the equilibrium quantities are constant along field lines. Normally, equilibrium quantities change along field lines, which may have an important effect on plasma stability. To take this effect into account we next study the resistive MHD stability of the separable point dipole equilibrium by Krasheninnikov, Catto and Hazeltine described in Ref. [19].

Following Ref. [19], we introduce the spherical coordinates r, θ and ζ; the quantities $\mu \equiv \cos\theta$ and $R = r\sin\theta$;

$$\begin{aligned} \psi &= \psi_0\left(R_0/r\right)^{\lambda} h\left(\mu\right), \qquad p = p_0\left(\psi/\psi_0\right)^{2+4/\lambda}, \\ B &= B_0\left(\psi/\psi_0 h\right)^{1+2/\lambda} G\left(\mu\right), \qquad G\left(\mu\right) \equiv \left[h^2/\left(1-\mu^2\right) + \left(\lambda^{-1}\mathrm{d}h/\mathrm{d}\mu\right)^2\right]^{1/2}, \end{aligned} \tag{27}$$

and $\beta_0 \equiv 8\pi p_0/B_0^2$; where p_0, ψ_0 and $B_0 \equiv \lambda\psi_0/R_0^2$ are the values of plasma pressure, poloidal flux function, and magnetic field at a reference flux surface at $R = R_0$. The eigenfunction $h\left(\mu\right)$ and the eigenvalue λ depend on β_0 and are obtained by solving the Grad-Shafranov equation (A1) for the dipole plasma equilibrium. Using the preceding we can rewrite Eqs. (1) and (2) in the form

$$\begin{aligned} &\frac{\mathrm{d}}{\mathrm{d}\mu}\left[\frac{A\left(\mu\right)}{1+(\tilde{\eta}_{\|}/\tilde{\gamma})F\left(\mu\right)}\frac{\mathrm{d}\xi_{\psi}}{\mathrm{d}\mu}\right] - \left[\tilde{\beta}D\left(\mu\right)+\tilde{\gamma}^2C\left(\mu\right)\right]\xi_{\psi} = D\left(\mu\right)\tilde{W}, \\ &\frac{\mathrm{d}}{\mathrm{d}\mu}\left[\frac{A\left(\mu\right)}{F\left(\mu\right)}\frac{\mathrm{d}\tilde{W}}{\mathrm{d}\mu}\right] + \frac{\tilde{\eta}_{\|}}{\tilde{\gamma}}\tilde{\beta}D\left(\mu\right)\left[\tilde{W}+\tilde{\beta}\xi_{\psi}\right] = \\ &\tilde{\gamma}^2\left\{\left[H\left(\mu\right)+\left(1+\frac{\tilde{\eta}_{\perp}}{\tilde{\gamma}}F\left(\mu\right)\right)E\left(\mu\right)\right]\tilde{W} + \left[\frac{\tilde{\eta}_{\perp}-\tilde{\eta}_{\|}}{\tilde{\gamma}}\tilde{\beta}E\left(\mu\right)F\left(\mu\right) - \frac{D\left(\mu\right)}{\lambda^2}\right]\xi_{\psi}\right\}, \end{aligned} \tag{28}$$

with

$$A(\mu) \equiv \frac{h^{2-1/\lambda}}{(1-\mu^2)\,G^2}, \quad C(\mu) \equiv \frac{h^{2+5/\lambda}}{(1-\mu^2)\,G^2}, \quad E(\mu) \equiv \frac{h^{2+7/\lambda}}{G^2},$$

$$D(\mu) \equiv \frac{2h^{2+3/\lambda}}{G^2}\left[\frac{G}{h}\frac{\mathrm{d}}{\mathrm{d}\mu}\left(\frac{1}{G}\frac{\mathrm{d}h}{\mathrm{d}\mu}\right) - \frac{\lambda}{1-\mu^2}\right], \quad F(\mu) \equiv \frac{1}{h^{2/\lambda}\,(1-\mu^2)}, \tag{29}$$

$$H(\mu) \equiv \frac{2h^{3/\lambda}}{\Gamma\beta_0}, \quad \tilde{\beta} \equiv \frac{\beta_0\,(\lambda+2)}{\lambda}, \quad \tilde{\gamma} \equiv \frac{\gamma}{\gamma_A}\left(\frac{\psi_0}{\psi}\right)^{1+3/\lambda},$$

$$\tilde{\eta}_{\|,\perp} \equiv \frac{c^2 n^2 \eta_{\|,\perp}}{4\pi R_0^2 \gamma_A}\left(\frac{\psi_0}{\psi}\right)^{1+1/\lambda}, \quad \tilde{W} \equiv W\frac{\psi_0}{B_0^2}\left(\frac{\psi_0}{\psi}\right)^{1+4/\lambda}, \quad \gamma_A \equiv \sqrt{\frac{B_0^2}{4\pi\rho R_0^2}}.$$

As the point dipole equilibrium[19] is up-down symmetric about the equatorial plane, solutions of Eqs. (28) and (29) are either up-down symmetric (even) or antisymmetric (odd).

Determining the correct boundary conditions for the functions ξ_ψ and $\tilde{W}$ is difficult, as the equilibrium is singular at the point dipole position, $\mu = \pm 1$. In fact,

$$h(\mu) \to -h'(1)\,(1-|\mu|) \quad \text{as} \quad \mu \to \pm 1, \tag{30}$$

so that the magnitude of the magnetic field becomes infinite as $\mu \to \pm 1$. Consequently, in order to find the correct boundary conditions at $\mu \to \pm 1$ we first have to obtain solutions of Eqs. (28) in this limit. Using approximation (30) in Eqs. (29) and (28) we find, after some algebra, four linearly independent solutions:

$$\left\{ \begin{array}{l} \xi_{\psi 1}(\mu) \\ \tilde{W}_1(\mu) \end{array} \right. \approx \left\{ \begin{array}{c} 1 \\ \frac{|h'(1)|^{2/\lambda}\lambda}{2(2\lambda+3)}\left[\tilde{\gamma}^2 + \frac{\tilde{\eta}_\|}{\tilde{\gamma}}(\lambda+2)^2\beta_0^2\right](1-|\mu|)^{1+2/\lambda} \end{array} \right., \tag{31}$$

$$\left\{ \begin{array}{l} \xi_{\psi 2}(\mu) \\ \tilde{W}_2(\mu) \end{array} \right. \approx \left\{ \begin{array}{c} (1-|\mu|)^{1/\lambda} - \frac{\tilde{\eta}_\|}{\tilde{\gamma}}\frac{1}{2|h'(1)|^{2/\lambda}(\lambda+1)}(1-|\mu|)^{-1-1/\lambda} \\ \left[\tilde{\gamma}^2 + \frac{\tilde{\eta}_\|}{\tilde{\gamma}}(\lambda+2)^2\beta_0^2\right]\left[\frac{|h'(1)|^{2/\lambda}\lambda}{4(\lambda+3)}(1-|\mu|)^{1+3/\lambda} - \frac{\tilde{\eta}_\|}{\tilde{\gamma}}\frac{\lambda}{4(\lambda+1)}(1-|\mu|)^{1/\lambda}\right] \end{array} \right., \tag{32}$$

$$\left\{ \begin{array}{l} \xi_{\psi 3}(\mu) \\ \tilde{W}_3(\mu) \end{array} \right. \approx \left\{ \begin{array}{c} -\frac{|h'(1)|^{2/\lambda}\lambda^3}{2(2\lambda+3)}\left[|h'(1)|^{2/\lambda}(1-|\mu|)^{2+4/\lambda} + \frac{\tilde{\eta}_\|}{\tilde{\gamma}}(1-|\mu|)^{1+2/\lambda}\right] \\ 1 \end{array} \right., \tag{33}$$

and

$$\left\{ \begin{array}{l} \xi_{\psi 4}\left(\mu\right) \\ \tilde{W}_4\left(\mu\right) \end{array} \right. \approx \left\{ \begin{array}{c} -\frac{|h'(1)|^{4/\lambda}\lambda^3}{\lambda+3}\left(1-|\mu|\right)^{1+3/\lambda} - \frac{\tilde{\eta}_{\|}}{\tilde{\gamma}}\frac{|h'(1)|^{2/\lambda}\lambda^3}{2}\left(1-|\mu|\right)^{1/\lambda} \\ \left(1-|\mu|\right)^{-1-1/\lambda} \end{array} \right. , \qquad (34)$$

where only the leading terms are displayed.

Solution (34) is clearly unphysical, as it corresponds to an infinite perturbed pressure at the point dipole position, and must be suppressed at all times. The ξ_ψ solutions (31) and (32) can be identified as the even and odd solutions, respectively, of the ideal equation (4). The fact that solution (32) becomes singular at the point dipole position when $\tilde{\eta}_{\|} > 0$ should not be too disturbing as the singularity occurs only in a very narrow region (as $\tilde{\eta}_{\|} \ll 1$) where no plasma is allowed since the magnetic field is *infinitely large*. Consequently, solutions (31) and (32), respectively, are even and odd solutions of Eqs. (28) as $\mu \to \pm 1$. Finally, solution (33) must be used in a linear combination with solutions (31) and (32) to form the desired even and odd eigenfunctions that satisfy Eqs. (28) and the boundary conditions at $\mu \to \pm 1$ as well as at $\mu = 0$. Use of (33) clearly does not cause any problem in the case of even modes, but forces the perturbed plasma pressure to make a finite jump at the point dipole in the case of odd modes. This jump is quite understandable as plasma can not be pushed through the region of infinite magnetic field.

In summary, the boundary conditions as $\mu \to \pm 1$ are given by linear combinations of solutions (31) and (33) for even modes, and (32) and (33) for odd modes. The unwanted solution (34) must be suppressed. The boundary conditions at $\mu = 0$ (the equatorial plane of the dipole) are simply $\mathrm{d}\xi_\psi/\mathrm{d}\mu\big|_{\mu=0} = \mathrm{d}\tilde{W}/\mathrm{d}\mu\big|_{\mu=0} = 0$ for even modes, and $\xi_\psi\left(\mu = 0\right) = \tilde{W}\left(\mu = 0\right) = 0$ for odd modes.

Equations (28) with the appropriate boundary conditions have been solved numerically. The corresponding eigenfunctions and eigenvalues for the even and odd modes have been obtained, first for the ideal case and then for the resistive case. In Figs. 1(a) and 1(b) hierarchies of ideal even and odd modes, respectively, are shown in solid lines for $0 < \beta < 1$ and $\Gamma = 5/3$, where $\tilde{\omega} \equiv \mathrm{i}\,\tilde{\gamma}$ (recall that $\tilde{\gamma}^2 = -\tilde{\omega}^2$ is always real in the ideal case[20]). The corresponding solutions of Eq. (4), which neglects coupling to sound waves, are shown for reference as dashed lines. As can be seen, for the point dipole equilibrium with $\Gamma = 5/3$ all the ideal modes are stable. Except for the lowest even mode, straight lines coming out of the origin correspond to an hierarchy of consecutive sound waves for which $\tilde{\omega}^2 \propto m^2\beta$ [compare this to Eq. (22) for the Z pinch], where m can be associated with the number of zeros of W in the interval $0 \leq \mu < 1$. As in the Z pinch case, no sound wave has been found for which ξ_ψ and W have a constant sign everywhere along a closed field line. In fact, W has one zero for the lowest sound wave, two zeros for the second lowest sound wave and so on, as demonstrated by Fig. 2 where the eigenfunctions ξ_ψ and W are shown for the three lowest even and three lowest odd modes at $\beta = 0.5$.

The lowest even mode in Fig. 1(a) is the lowest shear Alfvén mode (and not the lowest sound wave). As a result, the lowest solid line practically coincides with the lowest dashed line. To check that this identification is correct we artificially make Γ go to zero. Then, for a sound wave $\tilde{\omega}^2$ always has to stay positive, but go to zero; while for the lowest shear Alfvén mode $\tilde{\omega}^2$ has to become negative as this mode is mainly stabilized by plasma compressibility which is proportional to Γ [see Eq. (4)]. The check has been performed for the lowest even mode at $\beta = 1$ and the corresponding results are shown in Fig. 3 for $1 < \Gamma < 5/3$. It can be seen that $\tilde{\omega}^2$ becomes negative if $\Gamma < \Gamma_{marg} \approx 1.46$ and the mode is marginally stable at Γ_{marg}. But the lowest shear Alfvén mode is an interchange mode at marginality, hence Eq. (19) applies. This equation can be rewritten for the point dipole equilibrium in the form

$$\frac{2\,(2+\lambda)}{3+\lambda} < \Gamma, \tag{35}$$

where for $\beta = 1$, $\lambda \approx 0.703$ and the left-hand side is approximately 1.46; which is consistent with Γ_{marg}.

Returning to Fig. 1 we see that higher sound waves interact with the shear Alfvén modes. To demonstrate this coupling Figs. 4(a),(b) and 4(c),(d) present the eigenfunctions at $\beta = 0.5$ of the strongly interacting seventh and eighth lowest even modes and fourth and fifth lowest odd modes, respectively. Notice that for adjacent modes, the eigenfunctions ξ_ψ are nearly identical, while the eigenfunctions W oscillate roughly out of phase. The curves $\tilde{\omega}^2$ vs. β in Fig. 1 can not "cross", so the sixth lowest even sound wave for $\beta \lesssim 0.5$ (the seventh lowest even mode) becomes the second lowest even shear Alfvén mode at $\beta \gtrsim 0.5$; and the seventh lowest even sound wave for $\beta \lesssim 0.5$ (the eighth lowest even mode) becomes the sixth lowest even sound wave at $\beta \gtrsim 0.5$; etc [see Fig. 1(a)]. The odd modes behave in a similar way [see Fig. 1(b)].

Next, Eqs. (28) have been solved with resistive terms retained. In Figs. 5(a) and 5(b), respectively, the resistive growth/decay rates are shown for the lowest even and lowest odd modes for $0 < \beta < 1$. In the figures, $\mathrm{Re}\,(\tilde{\gamma})$ due to $\left(\tilde{\eta}_\perp,\, \tilde{\eta}_\parallel\right) = (0.1,\, 0)$, $\left(\tilde{\eta}_\perp,\, \tilde{\eta}_\parallel\right) = (0,\, 0.1)$ and $\left(\tilde{\eta}_\perp,\, \tilde{\eta}_\parallel\right) = (0.196,\, 0.1)$ are shown in dashed, dashed-dotted and dotted lines, respectively. Notice that $\tilde{\eta}_\perp$ alone is stabilizing, $\tilde{\eta}_\parallel$ alone is destabilizing, while the standard relation[24] $\tilde{\eta}_\perp = 1.96\tilde{\eta}_\parallel$ is stabilizing for the lowest even mode and destabilizing for the lowest odd mode.

Resistive decay rates are found to be rather sensitive to mode coupling. As an example, Fig. 5(c) gives $\mathrm{Re}\,(\tilde{\gamma})$ for the eighth lowest even mode for $0 < \beta < 1$. As before, dashed, dashed-dotted and dotted lines show $\mathrm{Re}\,(\tilde{\gamma})$ due to $\tilde{\eta}_\perp$ only, $\tilde{\eta}_\parallel$ only, and $\tilde{\eta}_\perp = 1.96\tilde{\eta}_\parallel$, respectively. Notice from Fig. 1(a) that the seventh, eighth and ninth even modes interact strongly at β between 0.3 and 0.5. These interactions are reflected in Fig. 5(c) where the resistive decay rate due to $\tilde{\eta}_\perp$ sharply decreases, while the resistive decay rate due to $\tilde{\eta}_\parallel$ sharply increases in the coupling region. Notice that, unlike the case of the lowest even and odd modes, parallel resistivity is stabilizing at all $0 < \beta < 1$ for the eighth lowest even mode.

Finally, we consider the scaling of the resistive growth/decay rates with resistivity. For all the point dipole cases considered it has been found that $\mathrm{Re}\,(\tilde{\gamma})$ is proportional to the first power of resistivity. Figure 6 illustrates this point by showing $\mathrm{Re}\,(\tilde{\gamma})$ vs. $\tilde{\eta}_\parallel$ for the lowest odd mode for $\tilde{\eta}_\perp = 1.96\tilde{\eta}_\parallel$ and $\beta = 0.1$. It is important to realize that instability does not occur on the equilibrium resistive time scale, but rather occurs n^2 times faster, where $n < 200$ for LDX. Resistive modes with faster growth $\mathrm{Re}\,(\tilde{\gamma}) \propto \tilde{\eta}_\parallel^{1/3}$ are not found for the point dipole equilibrium because it has the special property that it is always stable with respect to ideal odd modes, consistent with the proof of Sec. II. The LDX experiment is expected to have this same property since it is designed to be stable to ideal odd modes.[2] More general toroidal equilibria would be expected to permit marginal ideal odd modes and will therefore be susceptible to resistive instabilities with growth rate $\gamma \propto \eta_{\|}^{1/3}$.

V. Conclusions

The resistive stability of plasma confined by an axisymmetric closed line poloidal magnetic field has been investigated using MHD theory with anisotropic resistivity. By considering the most unstable modes with large azimuthal mode numbers, the system of resistive MHD equations has first been reduced to a system of two coupled second order differential equations for the radial component, ξ_ψ, and divergence, W, of the plasma displacement. These equations take into account the stabilizing influence of plasma and magnetic compression, and retain shear Alfvén modes, sound waves, and resistive modes.

Recalling that strong resistive instabilities are only possible at ideal mode stability boundaries, we have concentrated next on up-down symmetric systems (like a magnetic dipole) with $\beta \sim 1$. We used the coupled equations to show that resistive instabilities with $\gamma \propto \eta_{\|}^{1/3}$ are always present at the ideal stability boundary for up-down antisymmetric modes, and are never present at the ideal stability boundary for interchange modes. This result is valid for all systems except for those with equilibrium quantities constant along field lines, like a Z pinch, where there are no resistive instabilities with $\gamma \propto \eta_{\|}^{1/3}$ at $\beta \sim 1$.

Next, Z pinch equilibria have been studied in detail. A fourth order polynomial dispersion relation for a Z pinch has been derived and studied separately for $m = 0$ and $m \neq 0$ modes, where m is the azimuthal mode number. It has been found that when $m = 0$ only a shear Alfvén mode is present. Parallel resistivity is unimportant for this mode, while perpendicular resistivity damps it when it is ideally stable. The damping rate is proportional to the resistivity. At the same time resistivity does not modify the $m = 0$ mode stability boundary, which is given by the usual ideal interchange stability condition. The $m \neq 0$ case is more complicated. In the absence of resistivity both sound waves and shear Alfvén modes are present and are strongly coupled at $\beta \sim 1$, but uncouple at $\beta \ll 1$. A sufficiently strong pressure gradient can destabilize these ideal modes. The stability condition is identical to the one derived by Kadomtsev[22] from the ideal MHD energy principle. Parallel or perpendicular resistivity can destabilize ideally stable $m \neq 0$ modes. The growth rate of the instability is again proportional to resistivity. However, the pressure gradient necessary for this to happen is sufficient to destabilize the ideal $m = 0$ mode so this resistive growth is of no concern. As expected from the analysis of Sec. II, no resistive mode has been found for a Z pinch at finite β with growth or decay rate proportional to (resistivity)$^{1/3}$. However, such unstable resistive modes have been found at the ideal stability boundary for $m \neq 0$ modes at very low β, but again they are of no importance as the ideal $m = 0$ mode is also unstable in this case.

Finally, the stability of the point dipole equilibrium has been investigated numerically for $0 < \beta < 1$. Up-down symmetric (even) and antisymmetric (odd) modes have been studied separately and hierarchies of coupled sound waves and shear Alfvén modes have been obtained. All the modes have been found to be ideally stable at $\Gamma = 5/3$, while the lowest even (shear Alfvén) mode, which is stabilized mainly by plasma compressibility, becomes unstable when $\Gamma < 1.46$. Effects of resistivity on stability have been investigated and no resistive instability with $\gamma \propto \eta^{1/3}$ has been found. This result is in agreement with the analytical predictions as the point dipole equilibrium is stable with respect to ideal odd modes. In fact, resistivity only acts to modify the frequency of existing ideal modes by adding a small imaginary part and changing slightly the real part, with all changes being proportional to resistivity. The imaginary corrections to the frequencies (or growth or decay rates) due to parallel and perpendicular resistivity have been obtained vs. β for the lowest even, lowest odd and the eighth lowest even modes. It has been found that perpendicular resistivity alone always leads to damping in these three cases, while parallel resistivity alone leads to growth of the lowest even and the lowest odd modes. Moreover, for the case of most interest, $\eta_\perp = 1.96\eta_\parallel$, parallel resistivity dominates and destabilizes the lowest odd mode, while the lowest even mode remains damped. The growth rate of the lowest odd mode is on the order of the resistive time scale, τ_{res}, which is n^2 times faster than the resistive evolution time scale of the equilibria. This growth is a factor of $(\tau_A/\tau_{res})^{2/3} \ll 1$ smaller than the resistive instability time scale if a marginal odd mode were possible, where τ_A is the Alfvén time. Mode coupling has been found to have a strong effect on the resistive decay rates, and is shown to be able to increase them by orders of magnitude.

Acknowledgement

The authors would like to thank Prof. Bruno Coppi for suggesting the investigation of resistive modes in dipoles.

This work was supported by U.S. Department of Energy Grant No. DE-FG02-91ER-54109 at the Massachusetts Institute of Technology.

Appendix A. Derivation of Ballooning Equations

This appendix presents a derivation of Eqs. (1) and (2). We linearize the MHD equation of motion about an equilibrium with pressure p, density ρ, magnetic field $\boldsymbol{B} = \boldsymbol{\nabla}\psi \times \boldsymbol{\nabla}\zeta$, and plasma current $\boldsymbol{J} = (\mathrm{d}p/\mathrm{d}\psi)\, cR^2 \boldsymbol{\nabla}\zeta$, where ζ is the toroidal coordinate and the poloidal magnetic flux ψ is determined by the Grad-Shafranov equation

$$\boldsymbol{\nabla} \cdot \left(\frac{\boldsymbol{\nabla}\psi}{R^2} \right) + 4\pi \frac{\mathrm{d}p}{\mathrm{d}\psi} = 0. \tag{A1}$$

We write the linearized equation as

$$\rho\gamma^2 \boldsymbol{\xi} = \frac{1}{c} \boldsymbol{J}_1 \times \boldsymbol{B} + \frac{1}{c} \boldsymbol{J} \times \boldsymbol{B}_1 - \boldsymbol{\nabla} p_1, \tag{A2}$$

where

$$\boldsymbol{J}_1 = (c/4\pi)\, \boldsymbol{\nabla} \times \boldsymbol{B}_1, \tag{A3}$$

$$\boldsymbol{B}_1 = \boldsymbol{\nabla} \times \left[\boldsymbol{\xi} \times \boldsymbol{B} - (c/\gamma) \left(\eta_\parallel \boldsymbol{J}_{1\parallel} + \eta_\perp \boldsymbol{J}_{1\perp} \right) \right], \tag{A4}$$

and

$$p_1 = -\boldsymbol{\xi} \cdot \boldsymbol{\nabla} p - \Gamma p \left(\boldsymbol{\nabla} \cdot \boldsymbol{\xi} \right), \tag{A5}$$

are the current, magnetic field and pressure perturbations, respectively. We also assume that any perturbed quantity, A, can be written in the form $A(\psi, \theta, \zeta) = \hat{A}(\psi, \theta)\, \mathrm{e}^{\gamma t - \mathrm{i} n \zeta}$, where θ is a poloidal coordinate, $n \gg 1$ is the azimuthal mode number, and $\hat{A}(\psi, \theta)$ is a slow function of ψ and θ.

We employ the following representations for $\boldsymbol{\xi}$ and $\boldsymbol{B}_1$:

$$\boldsymbol{\xi} = \frac{\xi_B}{B^2} \boldsymbol{B} + \frac{\xi_\psi}{|\boldsymbol{\nabla}\psi|^2} \boldsymbol{\nabla}\psi + \frac{\xi_\zeta}{|\boldsymbol{\nabla}\zeta|^2} \boldsymbol{\nabla}\zeta, \quad \boldsymbol{B}_1 = \frac{Q_B}{B^2} \boldsymbol{B} + \frac{Q_\psi}{|\boldsymbol{\nabla}\psi|^2} \boldsymbol{\nabla}\psi + \frac{Q_\zeta}{|\boldsymbol{\nabla}\zeta|^2} \boldsymbol{\nabla}\zeta. \tag{A6}$$

Assuming that $c^2 \eta_{\parallel,\perp}/4\pi R^2 \gamma \ll 1$, while $c^2 n^2 \eta_{\parallel,\perp}/4\pi R^2 \gamma = \mathrm{O}(1)$, we find to leading order in the $1/n$ expansion that the $\boldsymbol{B}$ component of Eq. (A4) gives

$$\xi_\zeta \approx 0. \tag{A7}$$

Retaining the next order corrections in the $1/n$ expansion leads to

$$\frac{Q_B}{B^2} \left(1 + \frac{c^2 n^2 \eta_\perp}{4\pi R^2 \gamma} \right) = -\left(\frac{\boldsymbol{\nabla}\zeta \cdot \boldsymbol{\nabla}\xi_\zeta}{|\boldsymbol{\nabla}\zeta|^2} + \frac{\boldsymbol{\nabla}\psi \cdot \boldsymbol{\nabla}\xi_\psi}{|\boldsymbol{\nabla}\psi|^2} \right). \tag{A8}$$

Similarly, the $\boldsymbol{\nabla}\psi$ and $\boldsymbol{\nabla}\zeta$ components of Eq. (A4) give to leading order

$$Q_\psi\left(1+\frac{c^2n^2\eta_\parallel}{4\pi R^2\gamma}\right)=\boldsymbol{B}\cdot\boldsymbol{\nabla}\xi_\psi,\quad Q_\zeta\left(1+\frac{c^2n^2\eta_\parallel}{4\pi R^2\gamma}\right)=\boldsymbol{B}\cdot\boldsymbol{\nabla}\xi_\zeta. \tag{A9}$$

Considering next the $\boldsymbol{\nabla}\zeta$ component of the momentum equation (A2) we obtain to leading order in $1/n$

$$Q_B+4\pi p_1\approx 0. \tag{A10}$$

Introducing

$$W\equiv-4\pi\left(p_1+\frac{\mathrm{d}p}{\mathrm{d}\psi}\xi_\psi\right) \tag{A11}$$

and using Eqs. (A1), (A6), (A8) and (A10) it is easy to find from Eq. (A5) that

$$\begin{aligned}\boldsymbol{B}\cdot\boldsymbol{\nabla}\left(\frac{\xi_B}{B^2}\right) &= \frac{1}{\Gamma p}\left[1+\frac{4\pi\Gamma p}{B^2}\left(1+\frac{c^2n^2\eta_\perp}{4\pi R^2\gamma}\right)\right]W\\ &+ \left[2\left(\frac{\boldsymbol{\kappa}\cdot\boldsymbol{\nabla}\psi}{R^2B^2}\right)+\frac{c^2n^2\eta_\perp}{\gamma R^2B^2}\frac{\mathrm{d}p}{\mathrm{d}\psi}\right]\xi_\psi.\end{aligned} \tag{A12}$$

In addition, using the expression for Q_ψ from Eq. (A9) and the definition of W, the $\boldsymbol{B}$ component of the momentum equation (A2) gives

$$\rho\gamma^2\boldsymbol{B}\cdot\boldsymbol{\nabla}\left(\frac{\xi_B}{B^2}\right)=\boldsymbol{B}\cdot\boldsymbol{\nabla}\left[\frac{\boldsymbol{B}\cdot\boldsymbol{\nabla}W}{B^2}\right]+\frac{c^2n^2\eta_\parallel}{4\pi\gamma}\frac{\mathrm{d}p}{\mathrm{d}\psi}\boldsymbol{B}\cdot\boldsymbol{\nabla}\left[\frac{(\boldsymbol{B}\cdot\boldsymbol{\nabla}\xi_\psi)}{R^2B^2\left(1+c^2n^2\eta_\parallel/4\pi R^2\gamma\right)}\right]. \tag{A13}$$

To form Eq. (1) we use the $\boldsymbol{\nabla}\psi$ component of the momentum equation (A2) along with the definition of W. Finally, using Eqs. (A12) and (A13) to eliminate ξ_B and Eq. (1) to rewrite the result, yields Eq. (2).

References

[1]J. Kesner, L. Bromberg, M.E. Mauel, and D. Garnier, 17th IAEA Fusion Energy Conference, Yokahama, Japan (International Atomic Energy Agency, Vienna, 1999), paper IAEA-F1-CN-69/ICP/09.

[2]D.T. Garnier, J. Kesner, M.E. Mauel, Phys. Plasmas **6**, 3431 (1999).

[3]A.N. Simakov, P.J. Catto, S.I. Krasheninnikov, J.J. Ramos, Phys. Plasmas **7**, 2526 (2000).

[4]J. Kesner, A.N. Simakov, D.T. Garnier, P.J. Catto, R.J. Hastie, S.I. Krasheninnikov, M.E. Mauel, T. Sunn Pedersen, J.J. Ramos, Nucl. Fusion **41**, 301 (2001).

[5]A.N. Simakov, R.J. Hastie, and P.J. Catto, Phys. Plasmas **7**, 3309 (2000).

[6]J. Kesner, Phys. Plasmas **5**, 3675 (1998).

[7]J. Kesner, Phys. Plasmas **7**, 3837 (2000).

[8]A.N. Simakov, P.J. Catto, and R.J. Hastie, Phys. Plasmas **8**, 4414 (2001).

[9]J. Kesner and R.J. Hastie, Phys. Plasmas **9**, 395 (2002).

[10]W. Horton, H.V. Wong, and J.W. Van Dam, J. Geophys. Res. **104**, 22745 (1999).

[11]W. Horton, H.V. Wong, J.W. Van Dam, and C. Crabtree, J. Geophys. Res. **106**, 18803 (2001).

[12]H.V. Wong, W. Horton, J.W. Van Dam, and C. Crabtree, Phys. Plasmas **8**, 2415 (2001).

[13]A.N. Simakov, R.J. Hastie, and P.J. Catto, Phys. Plasmas **9**, 201 (2002).

[14]B. Coppi, Phys. Rev. Lett. **22**, 50 (1969).

[15]H.P. Furth, J. Killeen, and M.N. Rosenbluth, Phys. Fluids **6**, 459 (1963).

[16]B. Coppi, J.M. Green, and J.L. Johnson, Nucl. Fusion **6**, 101 (1966).

[17]D. Correa-Restrepo, Z. Naturforsch. **37a**, 848 (1982).

[18]D. Correa-Restrepo, Z. Naturforsch. **45a**, 1074 (1990).

[19]S.I. Krasheninnikov, P.J. Catto, and R.D. Hazeltine, Phys. Rev. Lett. **82**, 2689 (1999).

[20]J.P. Freidberg, *Ideal Magnetohydrodynamics* (Plenum, New York, 1987).

[21]I.B. Bernstein, E.A. Frieman, M.D. Kruskal, and R.M. Kulsrud, Proc. R. Soc. London, Ser. A **244**, 17 (1958).

[22]B.B. Kadomtsev, in *Rewievs of Plasma Physics*, edited by M.A. Leontovich (Consultants Bureau, New York, 1965), Vol. 2, p. 153.

[23]M.N. Rosenbluth and C.L. Longmire, Ann. Phys. **1**, 120 (1957).

[24]S. I. Braginskii, in *Reviews of Plasma Physics*, edited by M. A. Leontovich (Consultants Bureau, New York, 1965), Vol. 1, p. 205.

Figure Captions

Figure 1. The hierarchies of (a) ideal even and (b) odd modes for the point dipole equilibrium at $\Gamma = 5/3$. Shown as dashed lines are the solutions of Eq. (4).

Figure 2. The eigenfunctions ξ_ψ and W, respectively, of Eqs. (1) and (2) with $\eta_\parallel = \eta_\perp = 0$ and $\beta = 0.5$ for the (a), (b) three lowest even and (c), (d) three lowest odd modes. The lowest, the second lowest and the third lowest modes are shown as dashed, dashed-dotted and dotted lines, respectively.

Figure 3. Stability of the lowest even (shear Alfvén) mode vs. Γ at $\beta = 1$.

Figure 4. The eigenfunctions ξ_ψ and W, respectively, of Eqs. (1) and (2) with $\eta_\parallel = \eta_\perp = 0$ and $\beta = 0.5$ for the strongly interacting (a), (b) seventh (dashed line) and eighth (dashed-dotted line) lowest even modes and (c), (d) fourth (dashed line) and fifth (dashed-dotted line) lowest odd modes.

Figure 5. Resistive growth rates for (a) the lowest even, (b) the lowest odd, and (c) the eighth lowest even modes. The dashed, dashed-dotted and dotted lines are the cases $\left(\tilde{\eta}_\perp, \tilde{\eta}_\parallel\right) = (0.1, 0)$, $\left(\tilde{\eta}_\perp, \tilde{\eta}_\parallel\right) = (0, 0.1)$ and $\left(\tilde{\eta}_\perp, \tilde{\eta}_\parallel\right) = (0.196, 0.1)$, respectively.

Figure 6. Linear scaling with resistivity of the resistive growth rate for the lowest odd mode at $\beta = 0.1$ for $\tilde{\eta}_\perp = 1.96\tilde{\eta}_\parallel$.

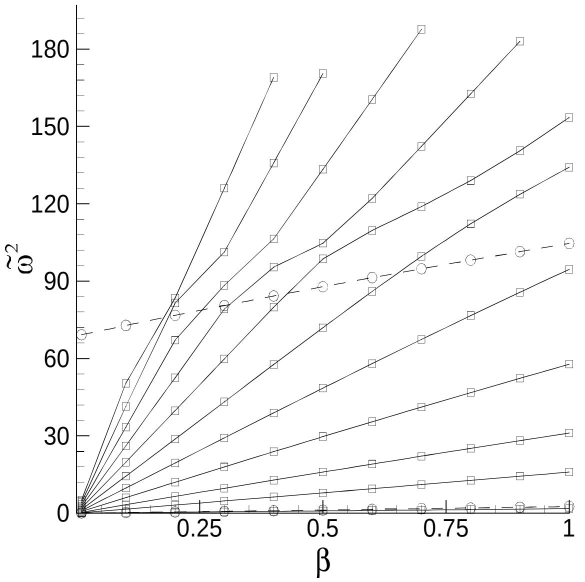

Figure 1(a)

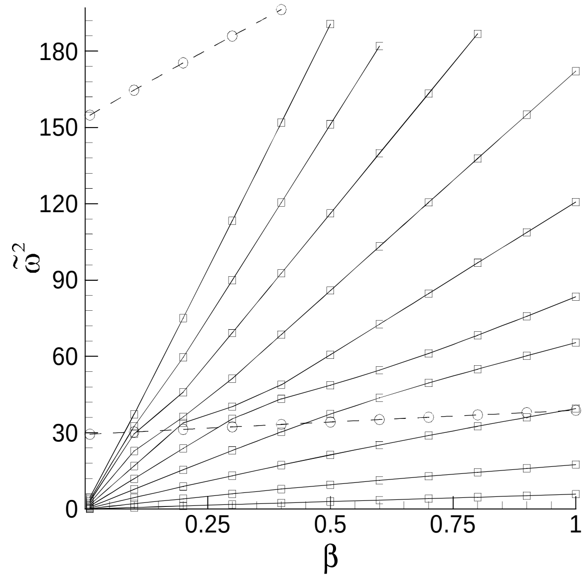

Figure 1(b)

A.N. Simakov, P.J. Catto, J.J. Ramos, and R.J. Hastie
Resistive Stability of Magnetic Dipole and Other
Axisymmetric Closed Field Line Configurations

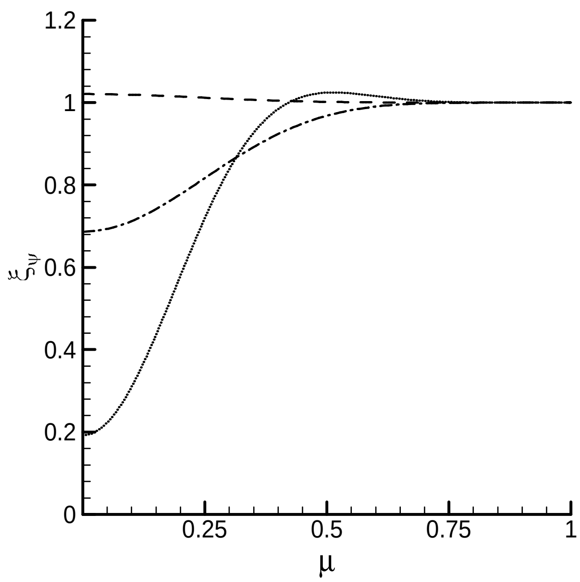

Figure 2(a)

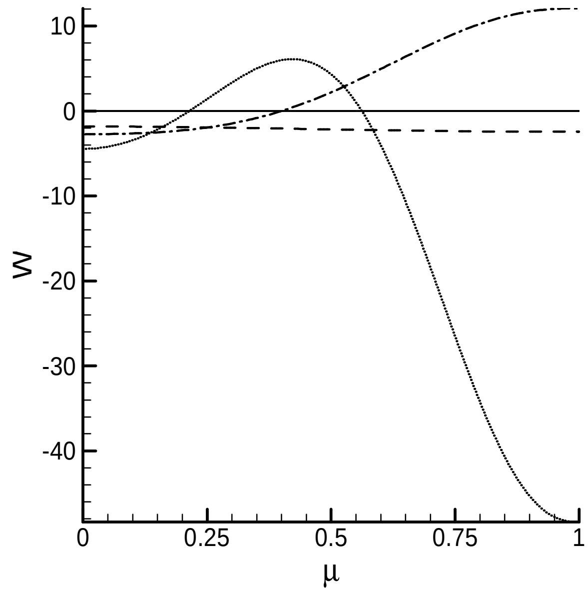

Figure 2(b)

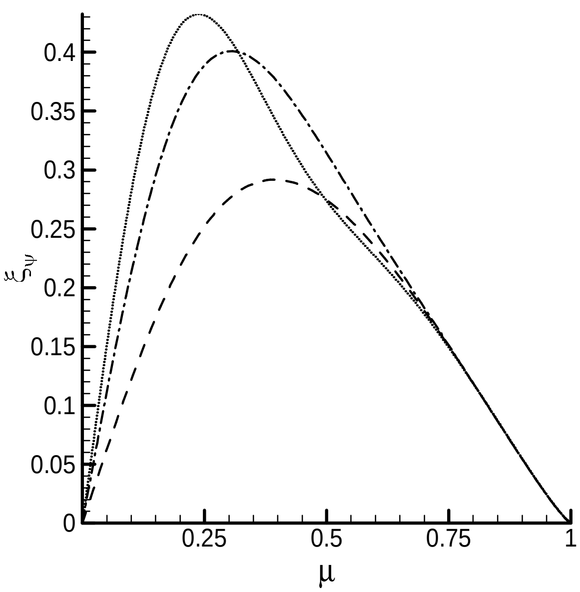

Figure 2(c)

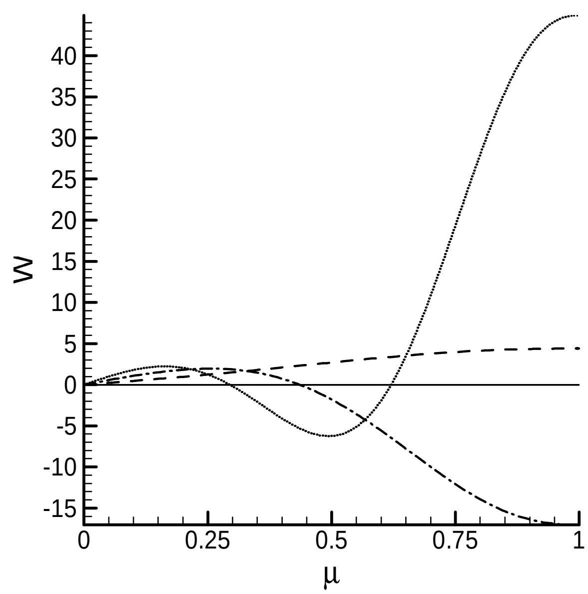

Figure 2(d)

A.N. Simakov, P.J. Catto, J.J. Ramos, and R.J. Hastie
Resistive Stability of Magnetic Dipole and Other
Axisymmetric Closed Field Line Configurations

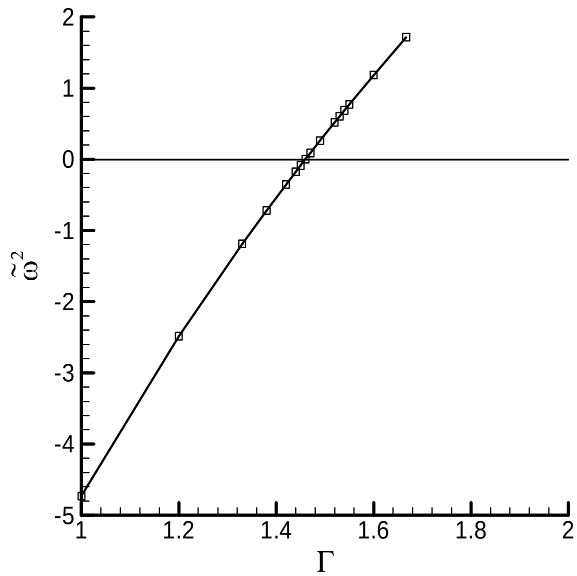

Figure 3

A.N. Simakov, P.J. Catto, J.J. Ramos, and R.J. Hastie
Resistive Stability of Magnetic Dipole and Other
Axisymmetric Closed Field Line Configurations

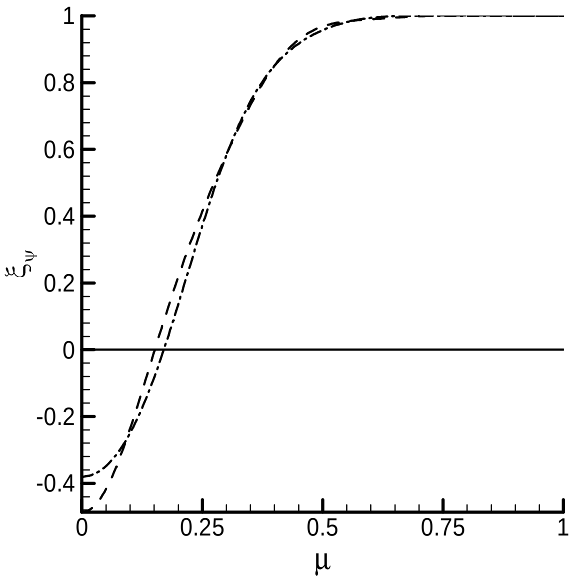

Figure 4(a)

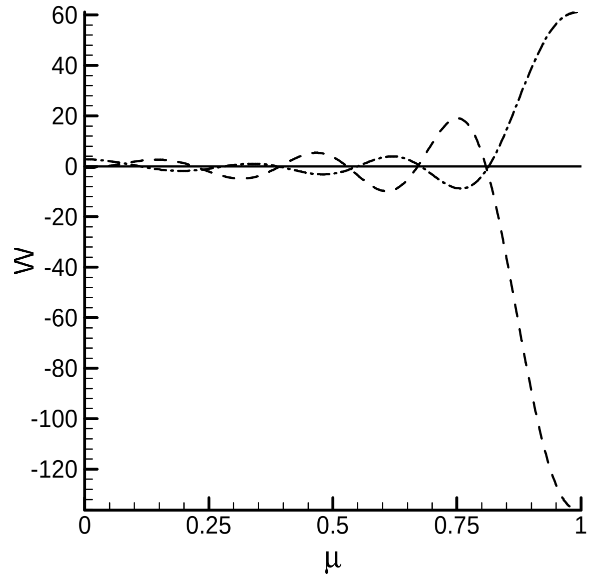

Figure 4(b)

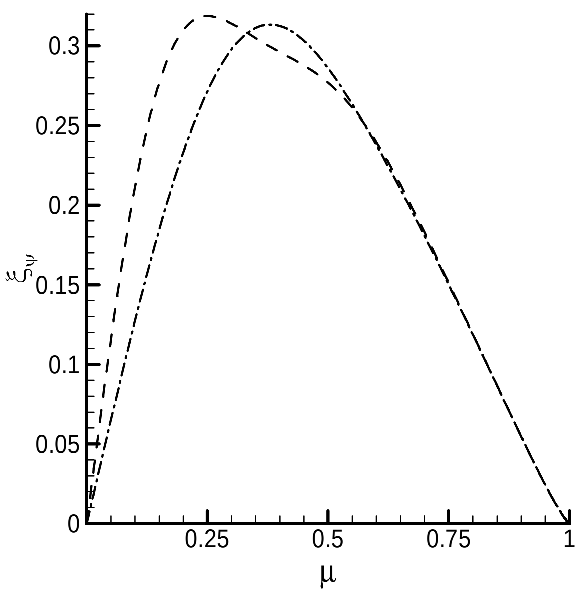

Figure 4(c)

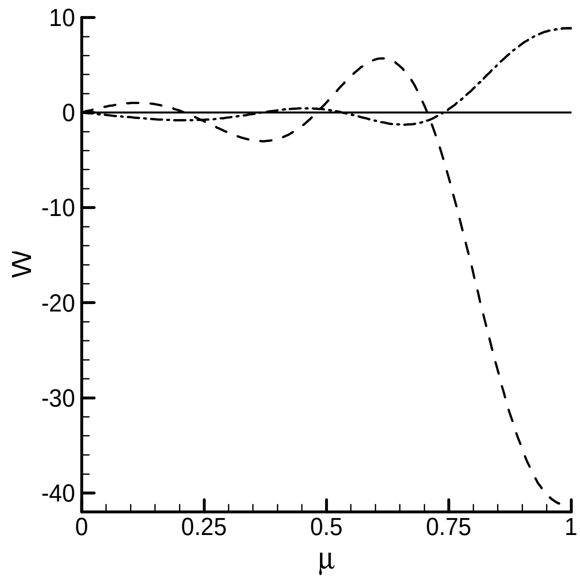

Figure 4(d)

A.N. Simakov, P.J. Catto, J.J. Ramos, and R.J. Hastie
Resistive Stability of Magnetic Dipole and Other
Axisymmetric Closed Field Line Configurations

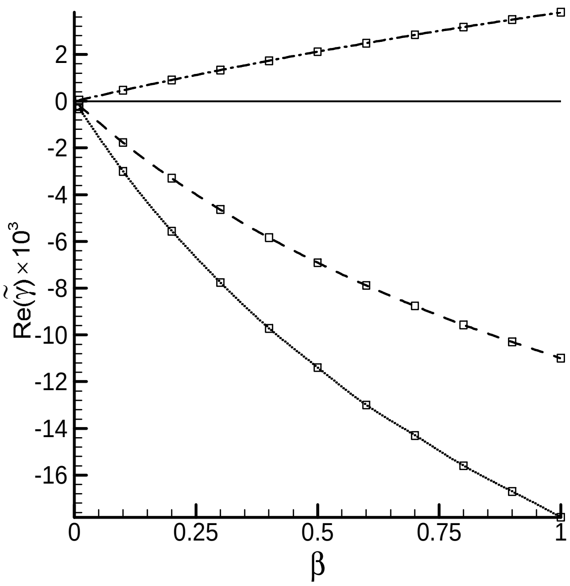

Figure 5(a)

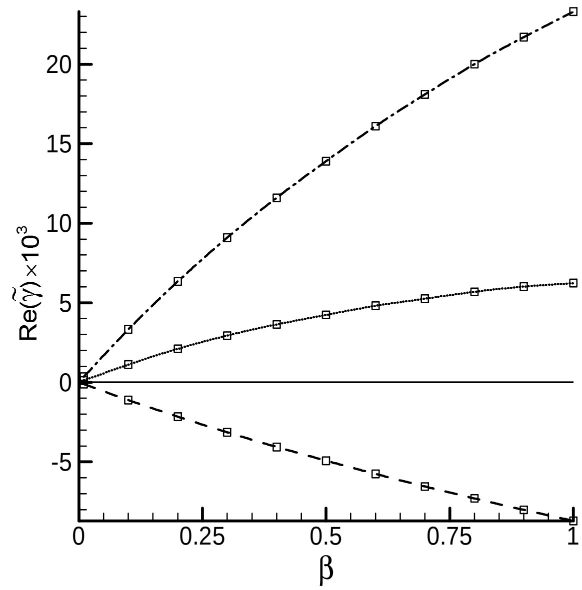

Figure 5(b)

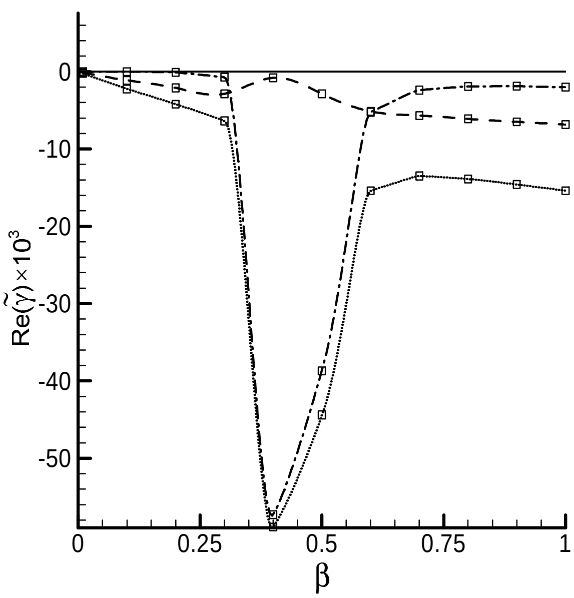

Figure 5(c)

A.N. Simakov, P.J. Catto, J.J. Ramos, and R.J. Hastie
Resistive Stability of Magnetic Dipole and Other
Axisymmetric Closed Field Line Configurations

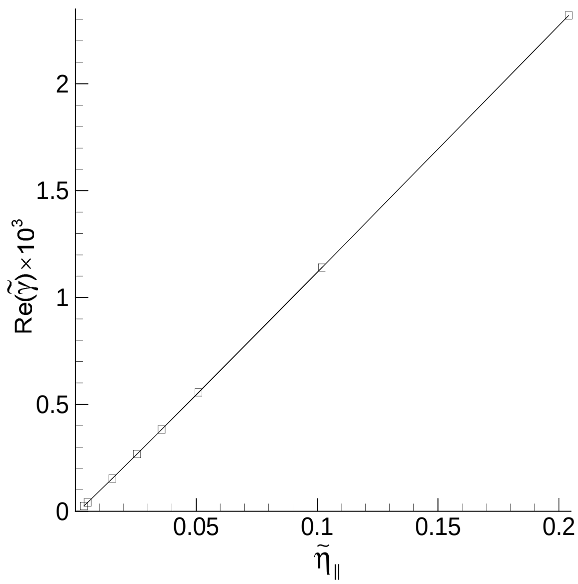
2
1.5
1
0.5
0
0.05
0.1
0.15
0.2
$\mathrm{Re}(\tilde{\gamma})\times 10^3$
$\tilde{\eta}_\parallel$

Figure 6